COMPUTATIONAL STUDY OF LAYER INVERSION IN TWO-COMPONENT LIQUID-FLUIDIZED BEDS BY DEM-CFD

Alberto Di Renzo[*]   Fernando Cello[†]

Francesco Paolo Di Maio[‡]

[*]Università della Calabria, Italy, alberto.direnzo@unical.it

[†]Università della Calabria

[‡]Università della Calabria

COMPUTATIONAL STUDY OF LAYER INVERSION IN TWO-COMPONENT LIQUID-FLUIDIZED BEDS BY DEM-CFD

Alberto Di Renzo, Fernando Cello, Francesco Paolo Di Maio
Dipartimento di Ingegneria Chimica e dei Materiali, Università della Calabria
Via P. Bucci, Cubo 44A, 87036 Rende (CS). Italy
T: +390984 496654, F: +390984 496655, E: alberto.direnzo@unical.it

ABSTRACT

In the present work the layer inversion phenomenon observed in experiments from the literature is reproduced via discrete element simulations, in which a novel drag force model valid for bi- and poly-disperse particle systems is used. The simulations serve both as validation of the drag model and as a tool to analyze the dynamics of the phenomenon. The comparison with published data is carried out in terms of bed height and component distributions as functions of the liquid velocity, showing very good agreement.

INTRODUCTION

Multi-component fluidization is used in several processes where each solid plays one or more specific roles (catalyst, inert, heat carrier, etc.). The presence of more species poses a number of fundamental and technological issues, mainly related to the non-uniform distribution of the components along the bed height. Due to the high number of variables involved, a full characterization of the mixing or segregation tendency of a given system is still an open problem.

One class of systems exhibiting a very peculiar behaviour is that giving rise to the so called "layer inversion" phenomenon. It occurs for certain solid pairs of a small dense and large light particles and is observed typically in liquid-fluidized beds. The two conditions among which these systems invert show one component predominantly accumulated at the top of the fluidized bed, above a layer of typically mixed composition or in extreme cases a layer of the other component fully segregated. The position of the two components may switch as a result of a change of fluid velocity or of the change of overall bed composition (i.e. by adding mass of one species). At the inversion point the two solids appear uniformly distributed throughout the whole bed. These systems have been studied by various authors in the literature (e.g. [1]), as recently reviewed by [2]. The slow dynamics and the uniformity of the flow field and voidage make it a very useful case for fundamental understanding of the governing factors and a key benchmark for model validation.

While many macroscopic models aimed at the prediction of the inversion conditions are available in the literature [2], detailed modelling efforts devoted to full flow simulation are very limited. Exceptions include Refs. [3-4] and recently Ref. [5], all based on a Two-Fluid Model approach. Another attempt is by Malone et al. [6], who

used Discrete Element Method (DEM-CFD) simulations to analyze an ideal binary, but no comparison with experiments was made, so no significant examples of particle-scale simulations of the inversion phenomenon are available.

With respect to the relatively simple simulation of the gas-fluidization of a single solids, in both modelling approaches two points deserve special attention, named the presence of a two-size suspension and the fact that more complex fluid-particle hydrodynamic interactions are typically present in highly dense and viscous liquids, e.g. lift, virtual mass, history integral (Basset) force and so on.

In the present work we use our coupled DEM-CFD model [7] with a recently proposed drag force model for bi- and poly-disperse solids [8] to simulate the inversion behaviour of a system studied by Matsuura and Akehata [9]. In analogy with a previous work on liquid-fluidization [10], we neglect at first interactions other than generalized buoyancy and drag, also in consideration of the fact that reliable expressions for various of the above contributions are available for isolated particles only.

The time required to carry out such simulations is so high that the focus will be only on one system, although other cases are currently under investigation. The selection of the binary in [9] results from the availability of all information required to set-up the simulation completely and the relative abundance of data to compare with. Detailed solid properties are available along with the temperature of the fluid (water), a key and often not reported variable that considerably influences the distribution of the solids. Also, apart from the overall bed height the position of the intermediate interface of the lower mixed zone was reported, making it possible to extend the analysis to the local distribution of the components inside the bed.

DEM-CFD MODEL

The DEM-CFD model we use is implemented within a FORTRAN90 code developed and extended during the last decade [7]. The code uses a rather standard coupled approach based on the particle-scale Discrete Element Method for the solid phase and a local-average CFD approach for the fluid phase. As in conventional DEM-CFD, the equation of translational motion is solved for each particle:

$$m_i \frac{d\mathbf{U}_i}{dt} = \sum_{j=1}^{Nc} \mathbf{F}_{c,ij} + \mathbf{F}_{d,i} + \mathbf{F}_{b,i} + \mathbf{F}_{g,i} \qquad (1)$$

where m_i and $\mathbf{U}_i$ are the i-th particle mass and velocity and the summation on the RHS includes contact forces $\mathbf{F}_{c,i}$ arising from the N_c contacts, the drag exerted from the fluid ($\mathbf{F}_{d,i}$), generalized buoyancy ($\mathbf{F}_{b,i}$) and gravity ($\mathbf{F}_{g,i}$), The contact force model was presented in Ref [11].

The expression for the drag force on a particle of species i was derived recently based on a large set of drag force data on individual particles from Lattice-Boltzmann simulations [8] as:

$$\mathbf{F}_{d,i} = \beta_i \overline{f} \cdot 3\mu\pi D_i u \qquad (2)$$

where the definitions of β_i and $\overline{f}$ are reported in Table 1. More details can be found in [8].

Table 1. Expressions for the average drag force and species factor in Eq. (2).

$$\overline{f} = K_1 + K_2 \cdot \varepsilon^4 + K_3 \cdot \left(1 - \varepsilon^4\right)$$

$$K_0 = \frac{1-\varepsilon}{1+3\varepsilon}; \quad K_1 = \frac{1 + 128K_0 + 715K_0^{\ 2}}{\varepsilon^2 \left(1 + 49.5K_0\right)}$$

$$K_2 = \frac{1 + 0.130\overline{\overline{Re}} + 6.66 \cdot 10^{-4}\overline{\overline{Re}}^2}{1 + 3.42 \cdot 10^{-2}\overline{\overline{Re}} + 6.92 \cdot 10^{-6}\overline{\overline{Re}}^2} - 1$$

$$K_3 = \left(\frac{2\overline{\overline{Re}}^2}{1+\overline{\overline{Re}}}\right)\left(\frac{-410\varepsilon + 9.20 \cdot 10^7 \overline{\overline{Re}} \cdot K_0^{\ 20} + 1900\varepsilon^2 - 6.60 \cdot 10^{-2} \cdot \overline{\overline{Re}}}{6600\varepsilon + 4.92 \cdot 10^{-4}\overline{\overline{Re}} - 43000\varepsilon^2 - 1.31 \cdot 10^{-4}\overline{\overline{Re}}^2 + 7.38 \cdot 10^4 \varepsilon^3}\right)$$

$$\beta_i = y_i + \frac{(1-\varepsilon)}{\varepsilon} \cdot \left(\frac{1-\varepsilon - 0.27}{1 - 0.27}\right) \cdot \frac{\left(y_i^2 - y_i\right)}{\displaystyle\sum_{k=1}^{Ns} x_k y_k}$$

with $\overline{D} = \left(\displaystyle\sum_{i=1}^{Ms} \frac{x_i}{D_i}\right)^{-1}$; $\overline{\overline{Re}} = \dfrac{\rho_f \, u\overline{D}}{\mu}$; $y_i = \dfrac{D_i}{\overline{D}}$; Ns is the number of species

Note: averaged properties like $\overline{D}$, $\overline{\overline{Re}}$ and the solid volumetric fraction x_i are evaluated at the computational cell scale.

Generalized buoyancy is

$$\mathbf{F}_{b,i} = -V_p \nabla P \qquad\qquad (3)$$

As mentioned in the Introduction other hydrodynamic force contributions are not considered.

The fluid phase flow field is solved on a local-averaged approximation of the continuity and Navier-Stokes equations with a scale of the order of the computational cell (typically a few particle diameters). Special care is devoted to ensure consistent coupling of drag force on individual particles and resistance source term that appears in the momentum balance equation for the fluid (see Ref. [8]).

Tools to analyse the layer inversion phenomenon

The simulations provide information on each single particle in the fluidized bed. However, to check the validity of the model against experimental data, post-processing of the local variables to get macroscopic quantities is necessary. Here two variables will be derived from the simulation results: the centres of mass of the two individual species and the height of the mixed layer in the bed. The former is used to assess the transient evolution of the solids distribution along the bed and to analyze the steady-state positions. The latter, together with the height of the overall bed, represent crucial parameters reported in the experiments which ideally serve as validation platform for the DEM-CFD simulations and the drag force in it. The height of the mixed layer is evaluated using the following procedure (Fig. 1). The time-averaged steady-state local concentration profile of species 2 $<x_2,loc>$ is calculated first. Then,
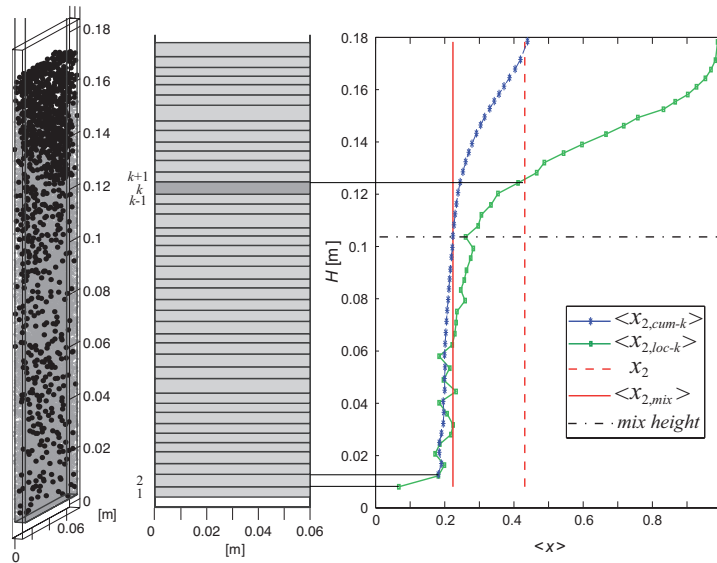
Figure 1. Schematic illustration and example of the technique used to evaluate the height of the mixed layer.

starting from the bottom of the bed, a local cumulative composition profile $<x_{2,cum}>$ is calculated at each height and when the height of the mixed layer is taken as the last layer whose local composition deviates from the corresponding cumulative value by more than 0.03.

DEM-CFD SIMULATIONS

Systems exhibiting layer inversion

The simulation of liquid-fluidized systems exhibiting layer inversion requires many data on the experimental conditions that are not always available in the literature. One of such key variables is fluid temperature as it is know to significantly influence the critical inversion conditions [2]. Also very useful for the purpose of comparing simulations and experiments are the equilibrium bed and mixed layer heights, which provide a rather strong basis for exploring the capability of the model to capture the correct expansion of the two solids both when mixed – at different compositions – and when isolated.

Considering the above requirements, of the various works available in the literature only few are potentially suitable for DEM-CFD simulations. We selected one of the systems investigated by Matsuura e Akehata [9]. Table 2 lists the properties of the original system used in experiments [9] as well as the data used to set-up the simulations. They are similar, with the exception of the geometry considered and the size. In the pseudo-2D geometry, the solid (DEM) is calculated in 3D with periodic boundaries in the thickness direction, the fluid flow (CFD) is considered only in the horizontal and vertical direction (2D). The column diameter is scaled down to 75% of its original size to lower the number of particles. The number of particles of the two species is 20400 for solid 1 and 1000 for solid 2. In the CFD a discretized domain involving 18x198 computational cells is used. The integration time step is $5 \cdot 10^{-6}$ s and the resulting CPU time is nearly five hours per simulated second on an Intel Xeon 3.0GHz server. Unfortunately, the characteristic time of the mixing or

Table 2. System properties in experiments [9] and simulations.

	Experimental system	Simulated system
Geometry	Cylindrical (3D)	Parallelepipedal (pseudo-2D) with periodic boundaries
System size	80 mm diameter	60 mm width x 4.01 mm depth
Particle diameters	0.807 mm (1), 2.010 mm (2)	
Particle densities	1395 kg/m^3 (1), 1170 kg/m^3 (2),	
Volumetric fraction	0.669 (1), 0.431 (2)	
Fluid properties	Water at 12-15°C	Density: 1000 kg/m^3; Viscosity: $1.14 \cdot 10^{-3}$ Pa s
Inlet velocities	5-40 mm/s	10,20,25,30,35,37 mm/s

segregation process in liquid systems is very high, so that in some of the simulations 300 seconds were necessary to achieve truly steady-state conditions.

RESULTS AND DISCUSSION

The reported experimental values of the velocity and voidage at the inversion conditions are u = 30 mm/s and ε = 0.87 [9]. The qualitative analysis of the results of the simulations performed using our polydisperse drag model at the different velocities (Table 2) shows that the component distribution along the system is consistent with the reported inversion conditions (Figure 2). Below the reported threshold velocity the larger and lighter component (black) is predominantly located on the top while at higher velocity the smaller component (grey) tends to accumulate to the top of the bed. These segregated conditions are more extreme as we move to the lowest and highest velocities, i.e. 10 mm/s (Figure 2a) and 37 mm/s (Figure 2f), respectively.
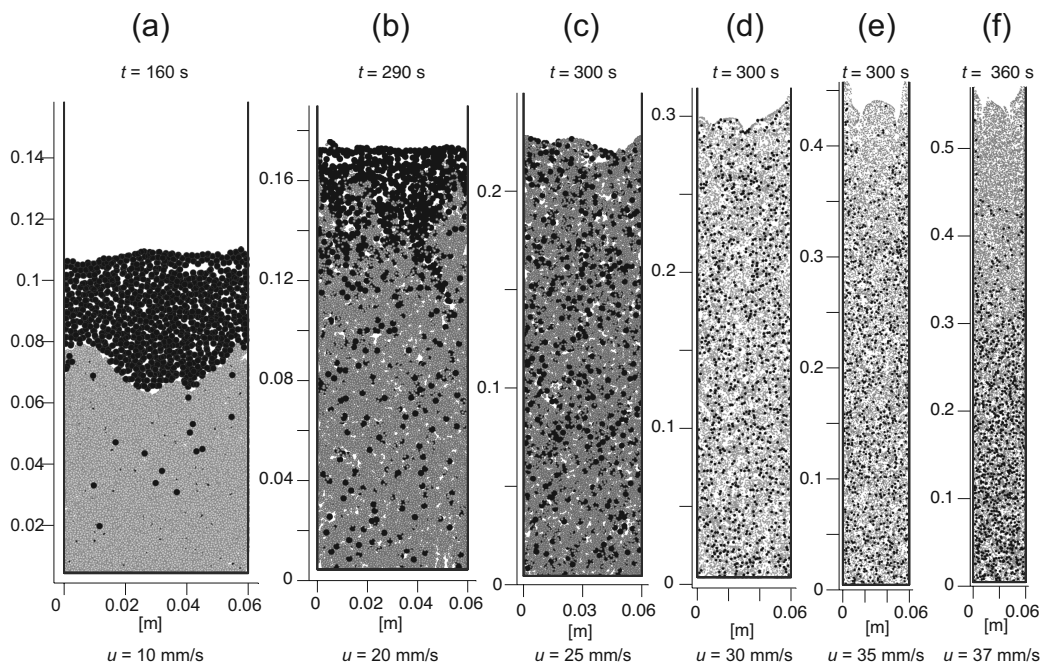

Figure 2. Steady-state particle positions along the fluidized bed. Solid 1 depicted in grey and solid 2 in black.
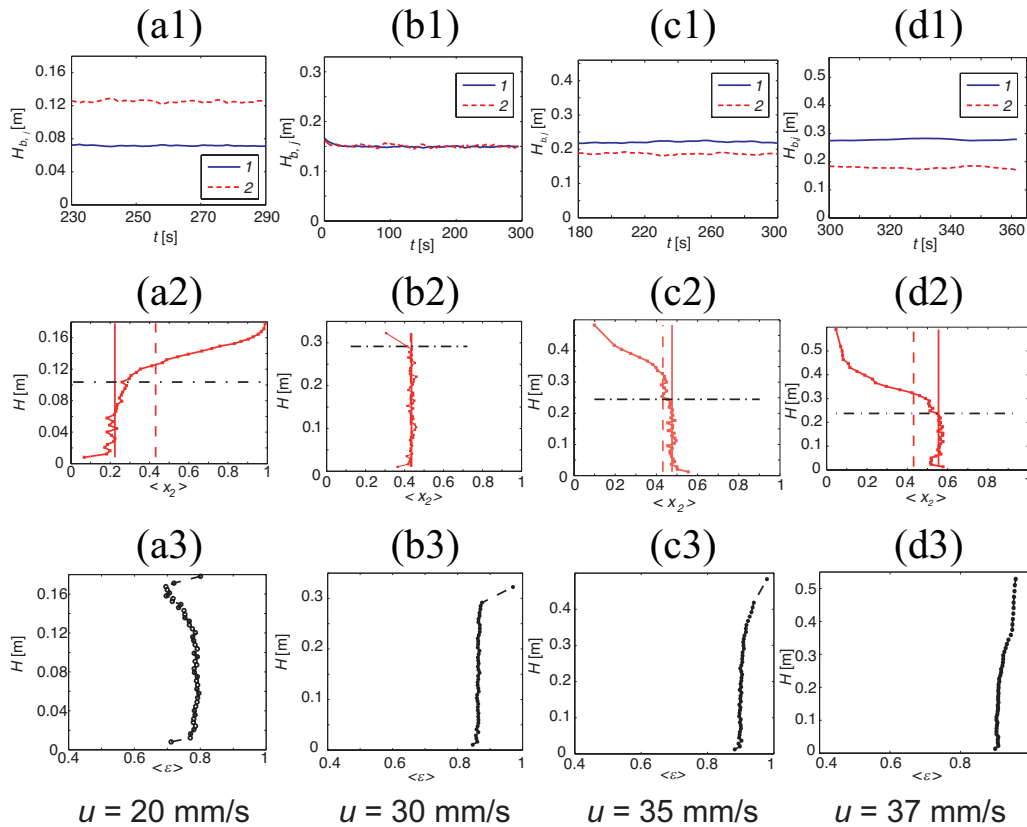
Figure 3. Results of the postprocessed simulations at 20 (a), 30 (b), 35 (c) and 40 mm/s (d). Transient evolution of the centres of mass of the two species (1), concentration profiles of species 2 with identification of the height of the mixed layer (2) and voidage profile along bed height(3).

A more quantitative analysis can be carried out by postprocessing the simulation results to get macroscopic quantities and profiles along bed height. Figure 3 shows such results for selected water velocities in terms of species centres of mass (Figure 3a1-3f1), time-averaged concentration profile of species 2 (Figure 3a2-3f2) and time-averaged voidage along bed height (Figure 3a3-3f3). The temporal evolution of the centres of mass of the species indicate that the two components have reached their equilibrium position in the bed.

All representations in Figure 3 confirm the presence of a clear layer inversion process and it is shown that almost perfect mixing and homogeneity is found at 30 mm/s and a voidage just below 0.9. The overall picture of the experiments seems very well predicted by the simulations. In Figures 3a2-3f2 the height of the mixed layer interface, calculated as described in section *Tools to analyse the layer inversion phenomenon*, is plotted along the composition profile. It is interesting to note that homogeneous expansion in terms of voidage is found only at the inversion conditions, while the presence of a mixed layer below and a segregated layer on the top causes a voidage profile to develop.

An accurate comparison of the expansion properties of the bed can be carried out against the reported experimental measurements [9], provided a scale-up of the simulation heights is performed using the same scale factor 0.75 of the geometry. The
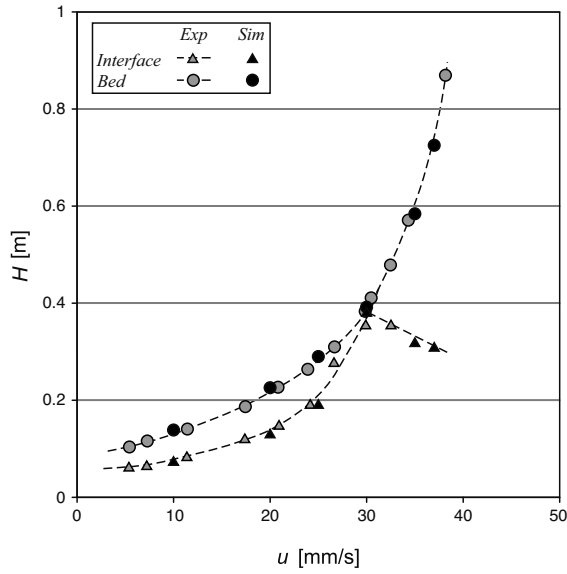
Figure 4. Comparison of scaled simulation results and experiments [9] in terms of bed and mixed layer interface heights versus inlet velocity.
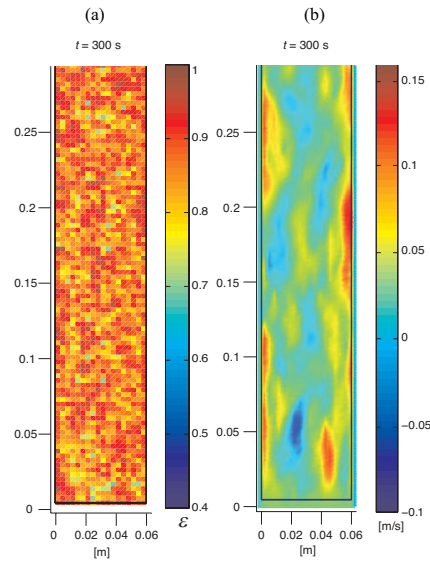
Figure 5. Snapshots of the steady-state voidage (a) and velocity (b) at the inversion velocity 30 mm/s.

scaled overall bed height and the height of the mixed layer predictions result in surprisingly good agreement with the experimental data (Figure 4). Despite the approximations in the approach and in the polydisperse drag model, the expansion behaviour of both species is captured with remarkable fidelity.

The inversion conditions are peculiar for their characteristics of homogeneity. As shown in the snapshots in Figure 5, the bed shows little and random variations of the voidage, while the velocity field exhibits higher values spuriously along the side walls. A final note concerns the importance of the proposed drag force model in the determination of the critical inversion conditions. To assess the influence of the drag
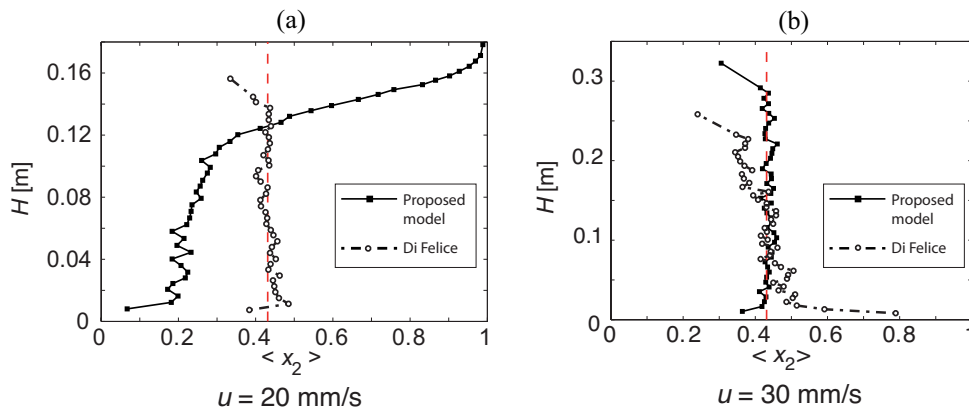

Figure 6. Time-averaged concentration of solid 2 along bed height resulting from simulations based on the proposed drag model and the model of Di Felice [12] at 20 (a) and 30 mm/s (b).

model we carried out simulations of the same system at 20 and 30 mm/s but using the drag model of Di Felice [12], typically used in DEM-CFD simulations of monodisperse systems. The steady-state composition profiles at the two velocities are represented in Figure 6. It is clear that such a drag model predicts the inversion conditions around the lower velocity instead of the higher value, with a significant deviation from full mixing at the true inversion velocity. Also, with reference to the data in Figure 4, at the inversion velocity the overall bed scaled height would be about 0.31 m against an experimental value of 0.41. This comparison highlight the influence of the drag model and emphasises the need of an accurate account of the polydispersion in the system for a correct evaluation of the fluid-particle interaction.

CONCLUSIONS

A set of DEM-CFD simulations of a liquid-fluidized bed of two solids exhibiting layer inversion has been carried out, with a novel drag force model applicable to polydisperse suspensions. The system was selected from the literature for the number of available data useful for comparison with the simulations. Steady-state overall bed height as well as mixed layer height at different velocities have been computed and the comparison with experiments shows a remarkably good agreement. Voidage and composition profiles were analyzed to fully describe the governing phenomena. A comparison with simulations using a traditional drag model demonstrates the importance of fully accounting for the size difference in all conditions.

REFERENCES

1. Moritomi H., Iwase T. and Chiba T., 1982. *Chem. Eng. Sci.* 37 (12),
2. Escudié R., Epstein N., Grace J. R. and Bi H. T., 2006. *Chem. Eng. Sci.* 61, 6667-6690.
3. Syamlal M. and O'Brien T. J., 1988. *Int. J. of Multiphase Flow* 14, 473-481.
4. Howley M.A. and Glasser B.J., 2002. *Chem. Eng. Sci.* 57, 4209-4226.
5. Reddy R.K. and Joshi J.B., 2009. *Chem. Eng. Sci.* 64 (16), 3641-3658.
6. Malone K.F., Xu B.H. and Fairweather M., 2007. *Fluidization XII*, 297-304.
7. Di Renzo A., 2004, *PhD thesis*, University of Calabria.
8. Cello F., Di Renzo A., Di Maio F.P., 2010. *Chem. Eng. Sci.* (to appear)
9. Matsuura A. and Akehata T., 1985. *50TH Annual Meeting of Society of Chemical Engineers of Japan* C-108.
10. Di Renzo A. and Di Maio F.P., 2007. *Chem. Eng. Sci.* 62 (1-2), 116-130.
11. Di Renzo A. and Di Maio F.P., 2005. *Chem. Eng. Sci.* 60 (5), 1303-1312.
12. Di Felice R., 1994. *Int. J. of Multiphase Flow* 20, 153-159.
13. van der Hoef M.A., Beetstra R. and Kuipers J.A.M., 2005. *J. of Fluid Mech.* 528, 233-254.